

## 7 Tesla Transmit-Receive Array for Carotid Imaging: Simulation and Experiment

G. Wiggins<sup>1</sup>, B. Zhang<sup>1</sup>, Q. Duan<sup>1</sup>, R. Lattanzi<sup>1</sup>, S. Biber<sup>2</sup>, B. Stoeckel<sup>3</sup>, K. McGorty<sup>1</sup>, and D. K. Sodickson<sup>1</sup>

<sup>1</sup>Radiology, Center for Biomedical Imaging, NYU School of Medicine, New York, NY, United States, <sup>2</sup>Siemens Healthcare, Erlangen, Germany, <sup>3</sup>Siemens Medical Solutions USA Inc., New York, NY, United States

**Introduction:** Significant improvements in SNR can be obtained through the use of receive arrays optimized to particular regions of interest in the body. At 3 Tesla, substantial improvements in carotid imaging were achieved through the design of a dedicated 8 channel carotid receive array [1]. At higher fields transmit body coils are not routinely available, and uniform excitation in the body is difficult to achieve and is currently the subject of considerable research. Therefore any 7 Tesla coil must include transmit capability, which increases the complexity of the design. In addition, the complex twisted B1+ and B1- profiles in human tissue at high RF frequencies require full wave electromagnetic simulation to accurately predict the performance of any given coil design. By choosing a specific region of interest in the body we can attempt to optimize both the transmit and receive profiles of a coil design for that specific application. We have used such simulations to help design and build an eight channel receive array for carotid imaging at 7 Tesla and tested it in human imaging.

**Methods:** The design parameters for the coil are shown in Figure 1. The rectangular ROIs mark the average position of the carotid arteries observed in a number of subject scans. For simulation, a cylinder of 130mm diameter with dielectric properties of muscle tissue at 7T was used to represent the neck ( $\sigma = 0.7698$  S/m and  $\epsilon_r = 58.24$ ). The receive elements and transmit elements are simulated on cylinders 140mm and 170mm diameter respectively. B1+ and B1- fields were simulated using a current mode expansion with a dyadic Greens function formulation [2,3]. The B1+ field of a single rectangular surface coil was simulated, 67mm wide circumferentially and 74mm long. The complex B1+ maps were cloned, rotated and summed in complex addition to determine the transmit profile of various transmit array configurations, assuming that available RF power was split equally to all the elements. The receive array elements were 40 x 37mm. Simulated SNR maps were generated for a receive array consisting of 2 sets of 4 overlapped coils, one each side of the phantom. The simulated SNR was compared to the ultimate SNR for a coil of that diameter.

The elements of the constructed array were machined from FR4 circuit board. The circular receive array elements had an inner diameter of 45mm and a track width of 5mm. These were connected to Siemens 7T preamps (Siemens Healthcare, Erlangen, Germany) by 10cm lengths of coax. Preamp decoupling was implemented by transforming the input impedance of the preamp to an inductance at the coil, forming a resonance with the match capacitor [4]. A PIN diode detuning trap was constructed around a neighboring capacitor and bias current was supplied to it through the coax and bridged to the trap by a 0.27 nH inductor. The transmit elements were overlapped to null mutual inductance and were each broken in two places with diodes to provide detuning during the receive phase. Pin diode detuning was measured with a shielded decoupled probe loosely coupled to the coil by comparing the response for the coil when terminated with 50 Ohms compared to the coil detuned. Preamp decoupling was similarly measured by comparing the response with the powered preamp in place or with the preamp replaced by a 50 Ohm load. A similar receive-only array was constructed for 3T to provide SNR comparison. B1+ maps were generated in a phantom by stepping through RF pulse voltages in a series of GRE acquisitions. SNR maps were generated from a GRE sequence and an identical acquisition with no RF excitation. The B1+ maps were used to normalize the SNR by calculating the SNR that would be obtained if there was a 90 degree excitation everywhere in the sample. This was necessary to compare the 3T and 7T coils since the transmit excitation for the 7T coil was highly inhomogeneous.

**Results:** A number of different transmit array configurations were examined in simulation. A simulated B1+ map for the 4-element transmit array that was chosen shown in Figure 2. By deliberately rotating the transmit coil 10 degrees clockwise the carotid ROIs receive similar excitation. Figure 3 shows the geometry of the 8 channel array which was simulated, the SNR of the array, and the ratio of the array SNR to the Ultimate SNR. The array achieves as much as 77% of the Ultimate SNR in two ROIs. By rotating the receive coils 10 degrees anti-clockwise these regions can be placed where the carotid ROIs are defined. Figure 4 shows the construction of the 7T carotid coil. Close inspection will show that the receive coils are shifted to the left of center and the transmit coils to the right of center as viewed in these images. The unloaded to loaded Q ratio of the receive elements is 3.1. Receive coil detuning is better than -35 dB, and transmit coil detuning is better than -30dB. Figure 5 shows the normalized SNR maps for the 7T and 3T coil arrays. The SNR of the 7T array is more than 3 times that of the 3T array, a result that is surprising and must be confirmed with further testing.

**Conclusions:** Full wave simulations with the dyadic Greens function approach allowed us to explore a range of design options before constructing a 7 Tesla coil for carotid imaging. In particular we were able to predict the spatial distribution of the transmit and receive profiles of the coil elements, and take this into account in the design of the coil.

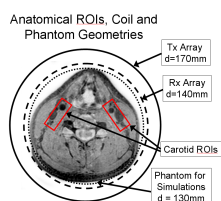


Figure 1

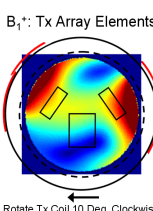


Figure 2

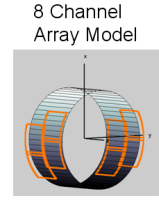


Figure 3

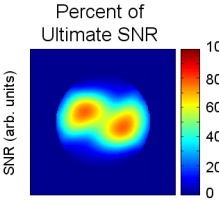


Figure 4



Figure 5

[1] Hinton-Yates et al, Top Magn Reson Imaging 2007, 18:5; 389-400

[2] Schnell, et al, IEEE TAP; 48:418-28.

[3] Lattanzi, et al, ISMRM 2008: 1074.

[4] Roemer et al Magn Res Med 1990 ;16 :192-225